Biodegradation (2006) 17: 303–316
DOI 10.1007/s10532-005-9000-3
© Springer 2006

Heterogeneous response to biostimulation for U(VI) reduction in replicated sediment microcosms

Jennifer L. Nyman[1], Terence L. Marsh[2], Matthew A. Ginder-Vogel[3], Margaret Gentile[1], Scott Fendorf[3] & Craig Criddle[1,*]
[1]*Department of Civil and Environmental Engineering, M42 Terman Engineering Center, Stanford University, 380 Panama Mall, Stanford, CA, 94305-4020, USA;* [2]*Microbiology and Molecular Genetics, Michigan State University, 2215 Biomedical Physical Sciences, East Lansing, MI, 48824-4320, USA;* [3]*Department of Geological and Environmental Sciences, Stanford University, 450 Serra Mall, Braun Hall, Building 320, Stanford, CA, 94305-2115, USA (*author for correspondence: e-mail: ccriddle@stanford.edu)*

Accepted 2 June 2005

Key words: 16S rDNA, bioremediation, subsurface, sulfate-reducing bacteria, T-RFLP, uranium reduction

Abstract

A field-scale experiment to assess biostimulation of uranium reduction is underway at the Natural and Accelerated Bioremediation Research Field Research Center (FRC) in Oak Ridge, Tennessee. To simulate the field experiment, we established replicate batch microcosms containing well-mixed contaminated sediment from a well within the FRC treatment zone, and we added an inoculum from a pilot-scale fluidized bed reactor representing the inoculum in the field experiment. After reduction of nitrate, both sulfate and soluble U(VI) concentration decreased. X-ray absorption near edge structure (XANES) spectroscopy confirmed formation of U(IV) in sediment from biostimulated microcosms, but did not detect reduction of solid-phase Fe(III). Two to three fragments dominated terminal restriction fragment length polymorphism (T-RFLP) profiles of the 16S rDNA gene. Comparison to a clone library indicated these fragments represented denitrifying organisms related to *Acidovorax*, and *Acidovorax* isolates from the inoculum were subsequently shown to reduce U(VI). Investigation using the T-RFLP Analysis Program (TAP T-RFLP) and chemical analyses detected the presence and activity of fermenting and sulfate-reducing bacteria after 2 weeks. These organisms likely contributed to uranium reduction. In some microcosms, soluble U(VI) concentration leveled off or rebounded, indicating microbial and/or mineralogical heterogeneity among samples. Sulfate, acetate, and ethanol were depleted only in those microcosms exhibiting a rebound in soluble U(VI). This suggests that rates of U(VI) desorption can exceed rates of U(VI) reduction when sulfate-reducing bacteria become substrate-limited. These observations underscore the importance of effective chemical delivery and the role of serial and parallel processes in uranium reduction.

Introduction

As a result of nuclear weapons production during the Cold War, soil and groundwater at numerous facilities within the Department of Energy (DOE) complex are contaminated with uranium (Riley et al. 1992). Remediation of such sites presents a challenge due to the lack of disposal facilities for radioactive waste generated during cleanup and because complex mixtures are present at some sites. Moreover, because uranium interacts strongly with solids, traditional groundwater remediation methods, such as pump and treat, may be cost-prohibitive or ineffective at reducing concentrations to low levels. A potential alternative is *in-situ* bioremediation (Lovley et al. 1991; Gorby & Lovley 1992). At the bench scale, the feasibility of such a strategy has been confirmed

with subsurface material (Abdelouas et al. 1998; Finneran et al. 2002b; Suzuki et al. 2003).

The fate and transport of uranium is governed by the contrasting chemistry of U(IV) and U(VI). U(VI) generally forms soluble, and thus mobile, complexes with carbonate and hydroxide, while U(IV) precipitates as the highly insoluble mineral uraninite. U(VI) can serve as an electron acceptor for certain iron-reducing, sulfate-reducing, homoacetogenic, and fermentative bacteria (Lovley et al. 1991, 1993; Francis et al. 1994; Suzuki et al. 2004), and U(IV) can serve as an electron donor with nitrate as an acceptor (Finneran et al. 2002a).

DOE has designated an area contaminated by the former S-3 ponds of the Y-12 facility in Oak Ridge, Tennessee, as a Field Research Center (FRC) for investigation of issues related to the *in-situ* bioremediation of metals. During nuclear weapons production at Oak Ridge, liquid uranium- and nitric acid-bearing wastes were discharged to a series of unlined surface ponds (the "S-3" ponds), and subsequent leaching from the ponds resulted in extensive contamination of the subsurface (http://www.esd.ornl.gov/nabirfrc/). A field-scale project is currently underway to evaluate the potential for bioreduction of uranium at an area adjacent to the former S-3 ponds. At this site, microbial uranium reduction is inhibited by the low pH (~3.4), high levels of calcium (Brooks et al. 2003), and high concentrations of nitrate (Finneran et al. 2002a; Senko et al. 2002). To alleviate these problems, a pretreatment strategy was implemented that involved flushing the contaminated region with acidified tap water to remove aluminum, reducing high bulk nitrate concentrations in a denitrifying fluidized bed reactor (FBR), and increasing the pH of the subsurface to a level suitable for microbial growth and the precipitation of calcium. Ethanol is currently being added to promote the *in-situ* denitrification of residual nitrate and to stimulate U(VI) reduction.

In this study, we used bacterial community fingerprinting and X-ray absorption near edge structure (XANES) spectroscopy to evaluate the potential for microbial uranium reduction in sediment from the site under conditions mimicking those of the field experiment. Denitrifying, fermenting and sulfate-reducing bacteria were implicated in the reduction of uranium. Although reduction occurred in most microcosms, in some, uranium was incompletely reduced, and soluble uranium concentrations either leveled off or rebounded. These differences were attributed to small-scale microbial or geochemical heterogeneities.

Materials and methods

Site description and sampling procedures

Aquifer sediment samples were collected from a site on the west side of the former S-3 disposal ponds, adjacent to the source zone of the contamination. The sampled well is currently used in the field experiment as an extraction well. The material at this site is primarily highly weathered shale and limestone (saprolite), and, at the time of sampling (i.e., prior to the initiation of remediation activities), the groundwater was characterized by low pH (~3.6) and high concentrations of nitrate, sulfate, volatile organic compounds, uranium, calcium, and aluminum (http://public.ornl.gov/nabirfrc/sumgwarea3.cfm). Cores were collected with a rotasonic drilling rig from well FW-103 on June 25, 2002. Subsections were transferred to sterile whirlpak bags and placed in ball jars under argon. Sediment samples from a depth of 12.2 m were shipped overnight to Stanford University and stored at 4 °C until use.

Microcosm preparation

Sediment and artificial groundwater were treated to simulate the treatment steps used in the field experiment. After pooling sediment (200 g) in a beaker, rocks were removed, and the sediment mixed with a spatula for homogenization while minimizing destruction of soil structure. The mixed sediment was then washed six times with 5 mM $CaBr_2$ and an additional time with denitrified synthetic groundwater (see below). Sediment and liquid were separated by centrifugation (6000 rpm, 20 min) between washes. The pH of the final wash water was 6.4. A portion of the washed sediment was preserved at 4 °C under a helium atmosphere for analysis by XANES spectroscopy, and a portion was frozen at −20 °C for bacterial community analysis.

Synthetic groundwater with aqueous chemistry analogous to site groundwater was prepared according to the following recipe: $Al(NO_3)_3$,

3.84 g/l; $Ca(NO_3)_2{\cdot}4H_2O$, 5.2 g/l; $NaNO_3$, 2.73 g/l; NaCl, 0.3 g/l; $MgSO_4$, 0.86 g/l; $MnSO_4{\cdot}H_2O$, 0.4 g/l; $CaCl_2$, 0.13 g/l; Na_2SO_4, 20 mg/l; KOH, 0.24 g/l. At the field site, groundwater passes through an aboveground treatment train that includes a pH increase to precipitate aluminum and calcium and denitrification in an FBR. Synthetic groundwater was prepared in an analogous manner. Nitrate was removed in a draw-and-fill batch reactor containing a denitrifying enrichment. The initial inoculum (430 ml) for the bioreactor was a denitrifying culture obtained from site groundwater amended with ethanol and lactate. The reactor received high-nitrate synthetic groundwater (40 ml, composition as described above) approximately every 10 days, along with 3 ml 1 M ethanol, 3 ml 1 M sodium lactate, and 0.6 ml $Na_3P_3O_9$. Denitrified water was withdrawn from the reactor for various experiments, resulting in a dilution rate of 0.01 d^{-1} (residence time of 100 days). The reactor was operated under these conditions for 10.5 months, and then for 1.5 months with ethanol as the sole electron donor (6 ml 1 M ethanol added every 10 days). Denitrification in the reactor increased the pH to approximately 7.1, causing precipitation of aluminum and calcium. Treated water was collected and centrifuged. Yeast extract was added to a final concentration of 16 mg/l and $Na_3P_3O_9$ was added to a final concentration of 0.22 mM to prevent nutrient limitations. The pH of the resulting solution was 7.54.

Microcosms were assembled in sterile anaerobic culture tubes (26.3 ml). Three grams washed sediment (dry weight) were added to each tube, followed by 10 ml denitrified synthetic groundwater. Each tube was inoculated with 5 ml effluent from a denitrifying FBR (Gentile et al. 2005). This step was included to simulate field operation, where a field-scale FBR is used for groundwater treatment. Ethanol and uranyl acetate were added to give final concentrations of 22 mM and 257 μM, respectively, from sterile, anaerobic stock solutions. The tubes were capped with butyl rubber stoppers and sealed, and their headspace purged with a N_2:CO_2 (80:20) gas mix.

A subset of the microcosms was sterilized by autoclaving and served as abiotic controls. All tubes were stored under quiescent conditions in the dark with daily mixing by inversion. Aqueous samples were withdrawn over time for U(VI) analysis, and sets of viable and control microcosms were sacrificed on days 1, 14, 27, 63, and 93 for more complete chemical, mineralogical, and microbial analyses. Sediment from replicates for a given time point was pooled and homogenized. One portion was preserved at 4 °C with a He headspace for XANES analysis; a second portion was preserved at −20 °C for bacterial community analysis.

U(VI) reduction by denitrifying isolates

Denitrifying isolates obtained from the FBR used as the source of added inoculum in the microcosm experiments were tested for their ability to reduce U(VI). Serial dilutions of effluent and homogenized biofilms were incubated aerobically at 30 °C on plates containing R2A, nutrient broth, Luria–Bertani (LB) medium, or filter sterilized reactor effluent supplemented with nitrate. Morphologically distinct isolates were picked, re-streaked to purity, and sequenced. Stocks of isolates were frozen at −80 °C in 20% glycerol. *Shewanella oneidensis* MR−1 was used as a positive control in U(VI) reduction experiments. Strain MR-1 was isolated from the anaerobic sediments of Oneida Lake, NY and is known to reduce U(VI) and grow with nitrate as a terminal electron acceptor (Myers & Nealson 1988; Lovley et al. 1991). The strain was obtained from Oak Ridge National Laboratory and stored as a freezer stock at −80 °C until use.

Four isolates (G1, G7, G17, and S3) were tested for their ability to reduce U(VI). Strains G1, G17, and S3 were closely related to *Acidovorax* sp. 3DHB1 (99% similarity), and G7 was most closely related to *Duganella zoogloeoides* (99% similarity) (Gentile et al. 2005). Similarity was based on homology of aligned 16S rDNA gene sequences. All four reduced nitrate to nitrogen gas (unpublished results). Frozen stocks were streaked onto Luria–Bertani (LB) agar (Difco) and grown at 30 °C overnight. Colonies from plates of the isolates and MR-1 were inoculated into 12 ml LB broth (Difco) and grown overnight at 30 °C on a flatbed shaker. Three tubes of each were combined and centrifuged at 6000 rpm for 20 min. The broth supernatant was decanted, and cultures were resuspended in 24 ml 30 mM sterile sodium bicarbonate. This washing procedure was repeated twice. Sterile serum bottles containing 45 ml media under a 80:20 N_2:CO_2 headspace were inoculated

with 5 ml resuspended culture in duplicate. The medium contained: $NaHCO_3$, 2600 mg/l; $NaNO_3$, 430 mg/l; Na_2SO_4, 4.7 mg/l; $MgCl_2{\cdot}6H_2O$, 7.0 mg/l; $CaCl_2{\cdot}2H_2O$, 10 mg/l; $Na_3P_3O_9$, 6.7 mg/l; sodium acetate, 370 mg/l; ethanol, 207 mg/l; and 0.3 ml of a trace element solution. The trace element solution contained: HCl, 6.4 ml/l; $FeCl{\cdot}4H_2O$, 0.3 g/l; $ZnSO_4{\cdot}7H_2O$, 0.1 g/l; $MnSO_4{\cdot}H_2O$, 0.085 g/l; HBO_3, 0.06 g/l; $CoCl_2{\cdot}6H_2O$, 0.019 g/l; $CuSO_4$, 0.004 g/l; $NiSO_4{\cdot}6H_2O$, 0.028 g/l; and $Na_2MoO_4{\cdot}2H_2O$, 0.04 g/l, and was modified from Widdel & Pfennig (1984). The pH of the inoculated bottles was 7.1 ± 0.1. Uranyl acetate was added from a sterile, anaerobic stock solution to give a final concentration of approximately 310 μM. It was also added to two anaerobic, sterile serum bottles containing 50 ml media, and these bottles served as abiotic controls. Bottles were stored under quiescent conditions in the dark at room temperature. Aqueous samples were taken anaerobically for U(VI) analysis immediately after the addition of uranium and after 29 and 116 days.

Analytical techniques

U(VI) was measured using a spectrofluorometer (Jobin Yvon Inc., Edison, NJ). Samples were diluted 1:30 in 10% phosphoric acid. The fluorescence of uranyl-phosphate complexes was measured at 515.4 nm in emission acquisition mode. All measurements were referenced to the fluorescence of the background matrix. Sulfate, acetate, nitrate, nitrite, and phosphate were measured in filtered samples on an ion chromatograph fitted with an AS11−HC column. Ethanol was measured in 0.03 mM oxalic acid by direct liquid injection to a gas chromatograph with a packed column (80/120 Carbopack B-DA/4% CARBOWAX 20M column) and a flame ionization detector. The concentration of U(VI) in the washed sediment was determined by anaerobically extracting 1 g sediment in 8 ml 1 M $NaHCO_3$ overnight and measuring the aqueous U(VI) concentration as described above (Elias et al. 2003). The measurement of sediment-associated U(VI) concentration was repeated in triplicate.

DNA extraction and amplification

DNA was extracted from preserved sediment samples with the UltraClean Soil DNA Kit (MoBio Laboratories, Solana Beach, CA). Approximately 1 g sediment was used in the extraction. DNA was extracted from the FBR inoculum and supernatant samples with the UltraClean Microbial DNA Isolation Kit (MoBio Laboratories, Solana Beach, CA) according to the manufacturer's instructions. The product was quantified by measuring the fluorescence of a DNA-dye complex on a Hoefer DyNA Quant 200 Fluorometer (Amersham Biosciences, Piscataway, NJ).

16S rDNA genes were amplified using the primer combination of 5-hexachlorofluorescein (HEX)-labeled 27f (5′-AGA-GTT-TGA-TCM-TGG-CTC-AG-3′) (Qiagen Operon, Alameda, CA) and unlabeled 1492r (5′-GGT-TAC-CTT-GTT-ACG-ACT-T-3′) (Qiagen, Alameda, CA) (Lane 1991). The standard reaction mixture contained the following in 100 μl: 1X PCR buffer (Promega, Madison, WI), 1.75 mM $MgCl_2$, 250 μM of each deoxynucleoside triphosphate, 0.38 mM forward primer, 0.25 mM reverse primer, 400 ng/μl bovine serum albumin (New England BioLabs, Beverly, MA), and 3 U of *Taq* DNA Polymerase (Promega, Madison, WI). DNA template was added at the concentration yielding the cleanest, brightest band upon gel electrophoresis of trial PCR reactions. Reactions mixtures were prepared on ice in 0.5-ml reaction tubes and transferred immediately to the preheated block (94 °C) of a PTC-150 MiniCyler (MJ Research, Waltham, MA). The thermal profile for the 16S rDNA amplification was as follows: initial denaturation (4 min at 94 °C) followed by 30 cycles of denaturation (94 °C for 40 s), annealing (56 °C for 40 s), and extension (72 °C for 90 s) with a terminal extension (72 °C, 7 min). Aliquots (5 μl) of amplicons were analyzed by gel electrophoresis on 1% agarose gels and visualized after UV excitation of ethidium bromide staining. The products of three PCR reactions were combined and purified with a Qiagen QIAquick cleanup kit (Valencia, CA), and DNA concentration was measured as described above.

T-RFLP

Amplified 16S rDNA was digested with restriction enzymes in 20-μl reactions containing the following: 1× reaction buffer (as recommended by the manufacturer), approximately 400 ng DNA, 10 μg/μl acetylated BSA (as recommended), and

5 U *Msp*I (Promega), 5 U *Hha*I (Promega), or 10 U *Rsa*I (Invitrogen, Carlsbad, CA). Reaction mixtures were incubated at 37 °C for 2.5 h for restriction enzyme digestion and subsequently at 65 °C for 10 min for enzyme inactivation. Products were stored at −20 °C and then shipped frozen to the Genomics Technology Support Facility (GTSF) at Michigan State University (MSU), where DNA fragments were separated by size by electrophoresis on an AppliedBiosystems 3100 Genetic Analyzer. The gel image was analyzed by correspondence to an internal standard with Genescan version 3.1 software (ABI).

Comparisons were made between profiles based on peak height. Total peak height was normalized as described by Dunbar et al. (2001), with the peak detection threshold set at 50. None of the peaks discussed in this study were discarded from any profiles through the normalization procedure. The DNA yield from the sediment sample from Day 63 was low and produced T-RFLP profiles of much lower total peak height than other samples, so it was not included in analyses. A list was compiled of fragment lengths that appeared during the course of the experiment and that comprised $>2\%$ of total peak height in at least one sample. T-RFLP Analysis Program (TAP T-RFLP), as described by Marsh et al. (2000), was used to perform an *in-silico* analysis of the expected fragment lengths resulting from digestion with *Msp*I, *Rsa*I, and *Hha*I. A window of ± 3 bp was used.

Cloning, sequencing, and phylogenetic analysis

16S rDNA was amplified from the FBR inoculum using the PCR conditions described above with the primers 27f (5′-AGA-GTT-TGA-TCM-TGG-CTC-AG-3′) (Qiagen Operon, Alameda, CA) and 1492r (5′-GGT-TAC-CTT-GTT-ACG-ACT-T-3′) (Qiagen, Alameda, CA) (Lane 1991). The concentration of forward and reverse primers in the reaction mix was 0.25 mM. A clone library was constructed with this DNA using the TOPO TA cloning kit, version Q (Invitrogen, Carlsbad, CA), according to the manufacturer's instructions. Plasmid inserts were sequenced by capillary electrophoresis on an AppliedBiosystems 3100 Genetic Analyzer by GTSF at MSU with the M13 forward primer. Sequences of 43 clones were checked for chimeras with the CHECK_CHIMERA program of the Ribosomal Database Project-II (Cole et al. 2003). Those with $>97\%$ sequence similarity were pooled, and representative sequences aligned with the RDP's Sequence Aligner. A phylogenetic tree was constructed using PHYLIP from the RDP with 443 bp of DNA sequence. Hypervariable regions were masked, Jin/Nei distances (coefficient = 0.1) between clonal and database sequences were calculated, and the tree was inferred with the Neighbor Joining method.

XANES analysis

XANES spectroscopy was used to determine the oxidation states of iron, chromium, and uranium. Sediment samples from the experiment were dried in an anaerobic glovebox, mounted on a Teflon plate, and sealed with Kapton polymide film to prevent oxidation while minimizing X-ray absorption. Samples were stored in the glovebox until analysis. XANES data were collected on beamlines 4–1 and 4–3 at the Stanford Synchrotron Radiation Laboratory (SSRL), running under dedicated conditions, and on beamline 13-BM-C (GSE-CARS) at the Advanced Photon Source (APS). The ring at SSRL operated at 3 GeV, with a current ranging from ~100 to 50 mA, while the APS ring operated at 7 GeV with a current of 100 mA. Energy selection at SSRL was accomplished with a water-cooled Si(220) monochromator, while a water-cooled Si(111) monochromator was used at the APS. Higher-order harmonics were eliminated by detuning the monochromator ~70% for Cr, ~50% for Fe, and ~10% for U in the absence of a harmonic rejection mirror. Fluorescence spectra were recorded by monitoring either the Cr K_α, Fe K_α, or the U $L_{III\alpha}$ fluorescence with a wide-angle ionization chamber (Lytle et al. 1984) for Fe or a 13-element Ge semiconductor detector for Cr and U. A Mn (for Fe) or Sr (for U) filter along with Soller slits was used to minimize the effects of scattered primary radiation, while no filter was used for Cr. Incident and transmitted intensities were measured with in-line ionization chambers. The energy range studied was -200 to $+500$ eV about the K_α-edge of Cr (6.989 keV) and Fe (7.111 keV) and the $L_{III\alpha}$-edge of U (17.166 keV). All spectra were collected at ambient temperature and pressure and 2–4 individual spectra were averaged for each sample.

Spectra were analyzed using IFEFFIT (Newville 2001) and WinXAS software (Ressler et al. 2000; Newville 2001). Fluorescence spectra were normalized, background subtracted, and the atomic absorption normalized to unity. First derivative XANES spectra were smoothed with a 17.6% Savitsky–Golay algorithm. The extent of downward shift in binding energy for a metal is related to its oxidation state, with a shift towards lower binding energy indicative of a lower oxidation state. XANES spectra of iron minerals shift downwards by 2–4-eV in energy with a decrease of one unit in valence (Waychunas et al. 1983; Kemner et al. 2001). Uranium XANES spectra shift downwards by ~4 eV in energy as valence decreases by two units, and the shoulder (multiple scattering resonance) on the high energy side of the main absorption feature of U(VI)-bearing phases is absent in U(IV)-bearing solids (Bertsch et al. 1994). Maxima of the first derivative of the XANES energies were compared between samples to assess the relative oxidation state of solid-phase iron, and the error in these determinations was approximately $+/-$ 0.5 eV. Site symmetry differences between Cr(VI) and Cr(III) allow the use of the pre-edge feature in the XANES spectra to quantify these two oxidation states (Patterson et al. 1997; Peterson et al. 1997).

The relative amount of reduced uranium in each sample was determined by fitting a series of Gaussian functions to the smoothed derivative spectra using PeakFit v4 (AISN Software Inc). The ratio of the amplitudes of the Gaussian functions centered at the U(IV) and U(VI) first derivative inflection points (17.172 and 17.176 keV, respectively) was related to U(IV)/(VI) proportions using five standards having U(VI) percentages ranging from 10 to 90%. The uncertainty of the fitting routine is $\pm 10\%$.

Results

Solution chemistry

Contaminated sediment was washed several times to neutralize its acidity and remove most solids-associated nitrate, simulating the flushing step in the field-scale experiment. Synthetic groundwater was biologically denitrified to remove most soluble nitrate and increase its pH, and this step approximated the aboveground process at the field site. Microcosms established with washed sediment and denitrified groundwater had an initial pH of 7.15, nitrate concentration of 1.1 mM, and nitrite concentration of 28 μM. Sets of viable and control microcosms were sacrificed over time for analysis, and the samples were labeled by the date on which they were sacrificed. Both nitrate and nitrite were depleted within the first 14 days in viable, but not control, microcosms (Table 1 and data not shown), indicating that the addition of the inoculum stimulated biological denitrification of residual nitrate.

Variable patterns of soluble U(VI) concentration over time were observed in viable microcosms (Figure 1). In most viable tubes, soluble U(VI) continually decreased (labeled D for decreasing), while in control microcosms U(VI) concentration was relatively steady. In other viable microcosms, soluble U(VI) concentration leveled off (labeled F for flattening) or rebounded (labeled ER for early rebound or LR for late rebound). The decrease in soluble U(VI) in viable but not control tubes indicated microbial activity was directly or indirectly responsible for the depletion.

In viable microcosms, most ethanol was depleted within 14 days (Table 1). This decrease in ethanol was accompanied by a concomitant increase in acetate, signifying that the ethanol was incompletely degraded. Acetate persisted throughout the experiment in most vials, except for those in which soluble U(VI) concentration rebounded. Sulfate concentration decreased in viable microcosms as well, but to varying degrees. It was only completely depleted in microcosms that exhibited a rebound in U(VI) and the complete depletion of acetate (Table 1).

Over time, pH decreased in both viable and control microcosms (Table 1), but in only the viable microcosms did a decrease in pH accompany a decrease in soluble U(VI). For a given pH, samples from viable tubes had lower U(VI) concentrations than those from control tubes (Figure 2). Of the viable microcosms, samples from Day 93 LR (late rebound) and ER (early rebound) had the highest pH after the first day.

Solids analysis

XANES spectroscopy was used to determine the average oxidation state of uranium, chromium, and iron associated with the sediment. Table 2 lists

Table 1. Electron donors, electron acceptors, and pH measured in the aqueous phase of microcosms sacrificed over time

Sample[a]	pH		Nitrate (mM)		Sulfate (mM)		Acetate (mM)		Ethanol (mM)	
	Control	Viable	Control	Viable	Control	Viable	Control	Viable	Control	Viable
Day 1	6.92	7.15	1.1 (0.04)[b]	0.1 (0.1)	3.3 (0.3)	3.0 (0.4)	bd[c]	bd	21.2 (2.6)	21.4 (3.7)
Day 14	6.77	6.69	1.0 (0.2)	0.04 (0.02)	3.2 (0.7)	0.1 (0.05)	bd	11.4 (1.0)	23.0 (3.9)	1.5 (0.8)
Day 27	6.68	6.59	1.6 (0.4)	bd	3.4 (1.3)	0.1 (0.2)	bd	13.5 (2.4)	21.7 (5.0)	bd
Day 63										
Decreasing	6.62	6.21	1.2 (0.1)	bd	4.1 (0.6)	2.3 (0.5)	bd	14.0 (2.1)	21.3 (1.5)	bd
Flattening		6.41		bd		1.7 (0.9)		13.2 (2.5)		bd
Day 93										
Decreasing	6.53	6.11	1.2 (0.2)	bd	4.0 (0.8)	2.7	bd	18.4	17.7 (1.9)	bd
Flattening		6.28		bd		1.4		28.3		bd
Early rebound		6.82		bd		bd		bd		bd
Later rebound		6.71		bd		bd		bd		bd

[a] Decreasing = decreasing pattern of soluble U(VI) concentration, Flattening = flattening pattern of soluble U(VI) concentration, Early rebound = early rebound of soluble U(VI) concentration, Late rebound = late rebound of soluble U(VI) concentration.
[b] Numbers in parentheses are one standard deviation.
[c] bd = below detection limit.
Values represent the average of replicates where available.

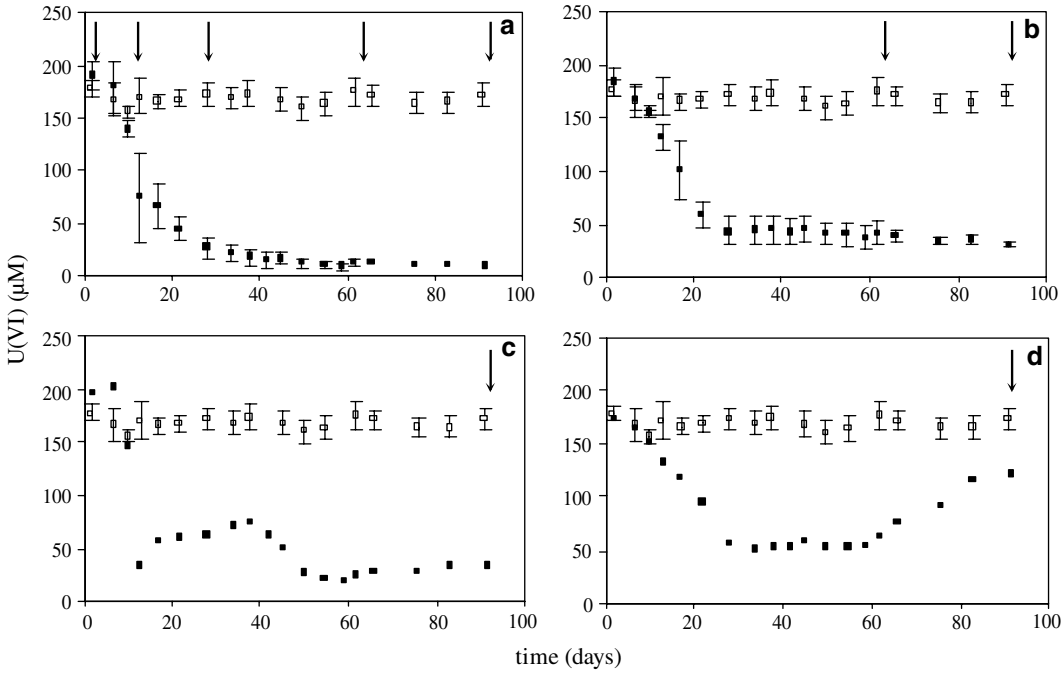

Figure 1. Variations in patterns of soluble U(VI) concentrations over time in source zone sediment microcosms. (a) Decreasing pattern (D), ($n = 10$). (b) Flattening pattern (F), ($n = 5$). (c) Early rebound pattern (ER), ($n = 1$). (d) Late rebound pattern (LR), ($n = 1$). Symbols: □, control (autoclaved) microcosms ($n = 15$); ■, viable microcosms. Error bars indicate one standard deviation, and arrows indicate days on which representative microcosms were sacrificed for more complete analysis.

the percentage U(IV) in sediment samples from sacrificed microcosms, and example spectra for uranium are displayed in Figure 3. Washed sediment originally contained 132 mg/kg dry weight uranium, as U(VI) (Table 2). Solid-phase uranium in sediment from control microcosms was initially

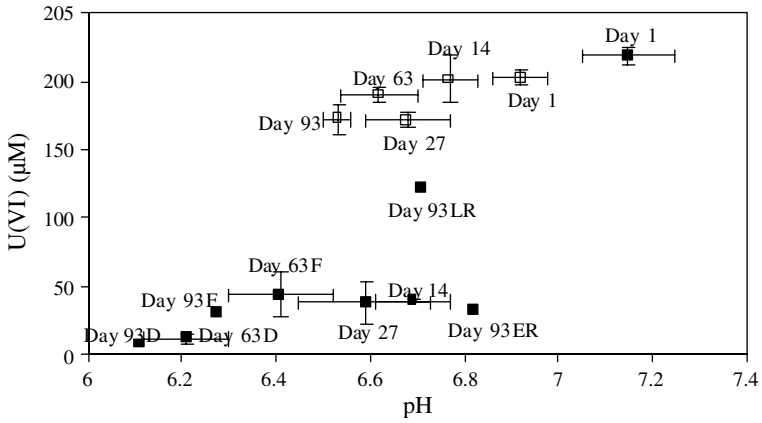

Figure 2. U(VI) concentration and pH in aqueous samples of sacrificed microcosms. Symbols: □, control (autoclaved) microcosms; ■, viable microcosms. Error bars indicate standard deviation ($n = 3$) where available, and data points are labeled with sample name.

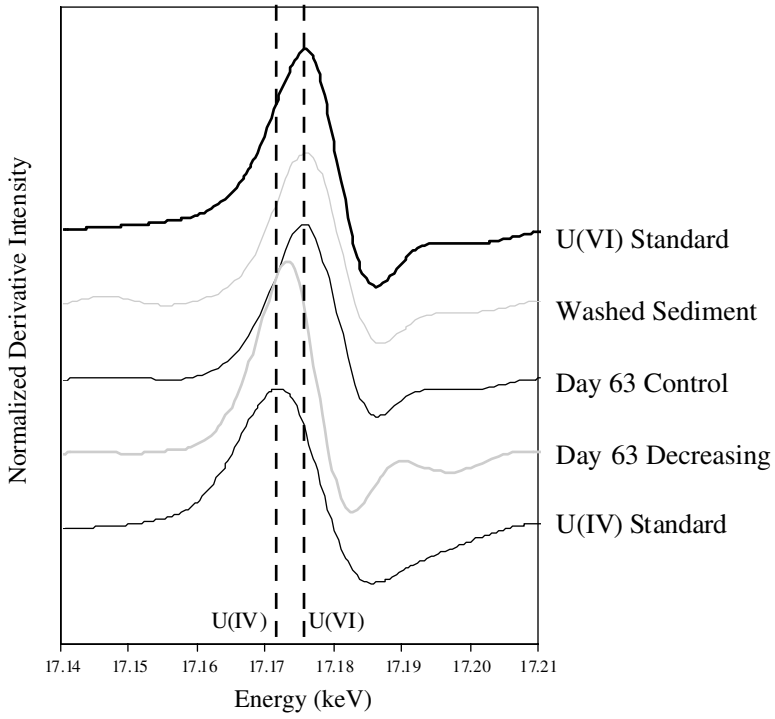

Figure 3. Example U(VI) XANES spectra of sediment from sacrificed microcosms, washed sediment initially added to microcosms, and uranium standards.

partially reduced, perhaps as an artifact of autoclaving, but with time for equilibration the uranium gradually oxidized. Uranium in sediment from viable microcosms, in contrast, typically became more reduced with time. Solid-phase Fe in control and viable microcosms was dominantly in the oxidized ferric-state throughout the experiment (data not shown). Normalized fluorescence spectra revealed the absence of an appreciable contribution of Cr(VI) within the samples and a prevalence of Cr(III) in an oxo or hydroxyl coordination environment (data not shown).

Table 2. Percent U(IV) in sediment samples from sacrificed microcosms, as determined by XANES analysis

Sample	Control	Viable
Day 1	57	20
Day 14	29	28
Day 27	22	40
Day 63		
Decreasing	0	62
Flattening		< 10
Day 93		
Decreasing	0	52
Flattening		0
Early rebound		10
Late rebound		< 10
U(VI) Standard	0	
U(IV) Standard	100	
Washed Sediment	0	

Community analysis

Sediment microcosms were inoculated with a denitrifying community developed from site groundwater. This same community served as an inoculum for the denitrifying FBR used in the field-scale experiment, and contains organisms whose growth could potentially be stimulated during field treatment. 16S rDNA genes were amplified from samples of the inoculum and sacrificed microcosms, and analyzed with T-RFLP using the enzymes *Msp*I, *Rsa*I, and *Hha*I. Initially, sufficient DNA for analysis was only recovered from the soluble phase (on Days 1 and 14). A small amount of DNA was obtained from the sediment on Day 14, but it did not yield enough PCR product for digestions with all three enzymes. From Day 27 onwards, DNA was recovered only from the sediment phase.

A histogram of each fragment length's contribution to total peak height of T-RFLP profiles for the enzyme *Msp*I is shown in Figure 4; similar results were obtained for *Rsa*I and *Hha*I. For each enzyme, one T-RF length (485 for *Msp*I, 423 for *Rsa*I, and 202 for *Hha*I) consistently had the greatest peak height for all microcosm samples, and this fragment length also represented the greatest proportion of peak height in the inoculum. The contribution of other fragment lengths to total peak height varied significantly between samples.

The phylogenetic relationship of clones from the inoculum to each other and related sequences from the RDP revealed that most clones (34) were closely related to *Acidovorax* species, eight were closely related to *Dechloromonas* species, and one was related to species of *Cytophaga* group I of the Cytophaga–Flavobacterium–Bacteroides (CFB) phylum (Figure 5). The *Acidovorax* and *Dechloromonas* genera contain denitrifying organisms

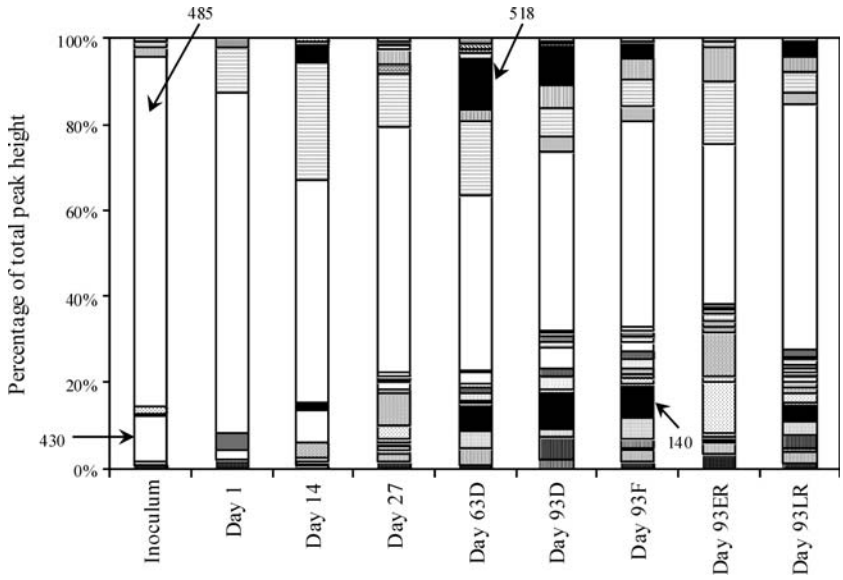

Figure 4. Individual peak contribution to total peak height of T-RFLP profiles for sediment from sacrificed microcosms digested with *Msp*I. Results were similar for *Hha*I and *Rsa*I. Selected fragment lengths are indicated.

(Kniemeyer et al. 1999; Schulze et al. 1999; Coates et al. 2001). The terminal restriction fragment (T-RF) lengths predicted from an *in-silico* digestion of sequences from the tree are also shown in Figure 5. Predicted fragment lengths for clones generally matched those for related, known sequences within one base pair, but predicted T-RFs were 3–4 bp longer than significant T-RFs detected experimentally. The predicted T-RF lengths of most *Acidovorax* species in the tree were 488 for *Msp*I, 427 for *Rsa*I, and 205 for *Hha*I, which are consistent with the prominent T-RF lengths of 485, 423, and 202 detected in experimental samples. The T-RF lengths 430, 117, and 205 for *Msp*I, *Rsa*I, and *Hha*I were prominent in the inoculum profiles, consistent with the presence of organisms related to *Dechloromonas* species (fragment sizes of 430, 120, and 207). T-RF lengths similar to those of the clone related to species of *Cytophaga* group I (84, 307, and 91 for *Msp*I, *Rsa*I, and *Hha*I) were detected in several sacrificed microcosms, but their contribution to total peak height was usually $< 3\%$.

Several T-RFs appeared during the course of the experiment and persisted in most subsequent samples. The identity of organisms contributing to these T-RFs was investigated using the phylogenetic analysis program TAP T-RFLP. TAP T-RFLP allows identification of organisms in the RDP based on the size of the expected terminal restriction fragments resulting from digestion of 16S rDNA. For a given restriction enzyme, many organisms will have fragments of the same size, but a three-enzyme fingerprint can be used for putative organism identification. In this work, fingerprints were generated the enzymes *Msp*I, *Rsa*I, and *Hha*I. Twenty-one organisms yielded fingerprints with lengths corresponding to those that appeared during the course of the experiment. The majority of these organisms were sulfate-reducing bacteria (*Desulfovibrio vulgaris*, *Desulfovibrio* sp. str. PT-2, *Desulfovibrio* sp. str. CVH2, *Desulfovibrio burkinensis* str. HDv, *Desulfovibrio senezii* str. CVL, and *Desulfobotulus* str. BG14) and fermenting bacteria (*Clostridium cellulovorans*, *Clostridium frigidicarnis*, *Clostridium tyrobutyricum*, *Clostridium proteolyticum*, and *Clostridium pasteurianum*). Fingerprints of sulfate-reducing bacteria correlated with the following T-RFs that appeared during the course of the experiment: 134, 135, 166, 286, and 498 for *Msp*I; 484, 486, and 488 for *Rsa*I; and 91 for *Hha*I. Fermenting bacteria correlated with the following: 518 for *Msp*I, 446 for *Rsa*I, and 226 for *Hha*I. No other genera of organisms appeared multiple times in the analysis.

U(VI) reduction by denitrifying isolates

Denitrifying isolates from FBR biomass, which was used as the inoculum in this experiment, were tested for their ability to reduce U(VI). As shown in Table 3, the three isolates related to *Acidovorax*

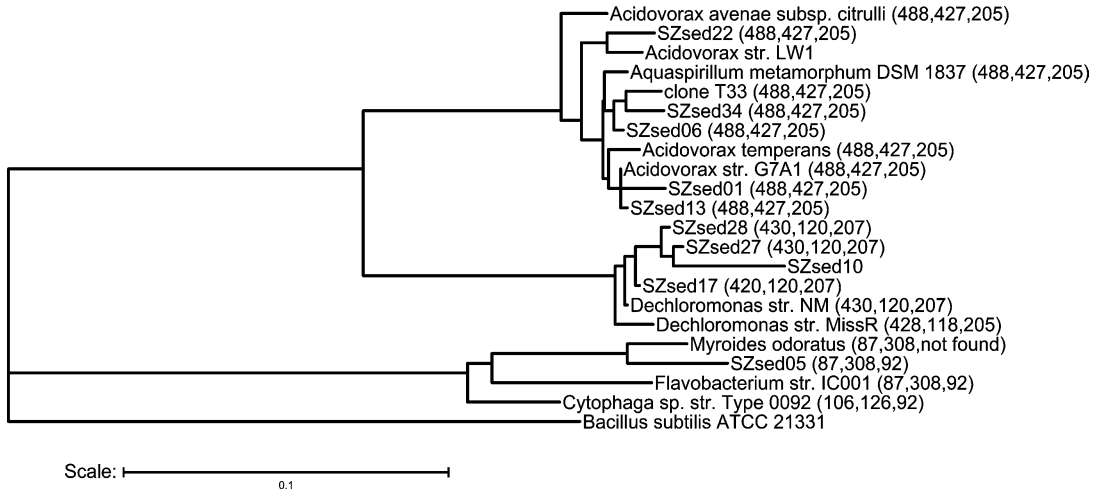

Figure 5. Clone library of FBR effluent sample used as an inoculum to the microcosms. The tree was constructed using 443 bp of DNA sequence. Only clones with less than 97% similarity are shown. Numbers in parentheses indicate restriction fragment lengths predicted from sequence data for *Msp*I, *Rsa*I, and *Hha*I, respectively, where distinguishable. Clones are name with the prefix "SZsed".

Table 3. Aqueous U(VI) concentration in bottles of denitrifying isolates

Sample	U(VI) (μM) Concentration			% U(VI) Reduced
	Day 0	Day 29	Day 116	
Isolate G1	309	222	177	43
Isolate G7	322	315	296	8
Isolate G17	329	200	151	54
Isolate S3	311	241	207	33
S. oneidensis MR-1	303	111	22	93
Abiotic control	322	333	324	—

species (isolates G1, G17, and S3) significantly reduced U(VI), while the isolate related to *Duganella* species (isolate G7) did not.

Discussion

Biostimulation at the Oak Ridge source zone

This work supported the potential for the field-scale immobilization of uranium at the source zone of the Oak Ridge FRC using ethanol as an electron donor. In the majority of microcosms with viable microbial activity (10 of 17), soluble U(VI) concentration continually decreased over time. The mechanism of removal was reduction, as established by XANES analysis of solid-phase uranium. Uranium was not reduced in sterilized microcosms, indicating that microbial activity mediated the observed reduction. After the first two weeks of incubation, DNA was recovered only from the solid phase, which suggests that organisms involved in U(VI) reduction were associated with the sediment.

For the source zone field experiment, clean, acidified water was first injected into the subsurface to displace high-aluminum groundwater. Groundwater was then pumped aboveground and its pH increased, resulting in the precipitation of remaining aluminum and calcium. The water was next treated in an FBR to remove nitrate, filtered, and injected into the subsurface. Because the filtration step was imperfect, we expect denitrifying organisms were added to the treatment zone in the reinjection step. Ethanol was then intermittently added to stimulate denitrification of residual nitrate and to promote U(VI) reduction. In the present experiment, these processes were simulated by washing the sediment with a salt solution, adding denitrified synthetic groundwater, inoculating with the effluent of an FBR, and amending with ethanol. As a result of these treatments, residual nitrate was depleted within the first two weeks (Table 1), and uranium reduction was observed. Shelobolina et al. (2003) incubated sediment from the Oak Ridge source zone with various electron donors to assess the potential for uranium bioremediation, but did not observe the reduction of uranium. This was most likely because at least 45 mM nitrate was present throughout the course of their experiment.

Community ecophysiology and uranium reduction

Several studies have described the ecology of U(VI)-reducing communities, and a wide variety of bacteria are apparently responsible for U(VI) reduction under different experimental and environmental conditions. U(VI) reduction has been observed during Fe(III) reduction in sediment microcosms (Finneran et al. 2002a, b; Nevin et al. 2003) and in field studies (Anderson et al. 2003; Istok et al. 2004), but in other experiments U(VI) reduction proceeded concurrently with sulfate reduction (Nevin et al. 2003) or with fermentation and sulfate reduction (Suzuki et al. 2003). Variation in the ecophysiology of U(VI)-reducers highlights the importance of evaluating each community under relevant environmental conditions.

In this work, one T-RF for each enzyme had the greatest peak height for all samples, and these prominent T-RFs likely corresponded to *Acidovorax* species from the denitrifying inoculum. Isolates from the inoculum, which can be tentatively classified as *Acidovorax*, reduced U(VI), suggesting that the organism with the most prominent T-RF may have reduced U(VI). This is the first report of U(VI) reduction by organisms closely related to *Acidovorax* species. We observed little denitrification beyond the first day, so these dominant T-RFs likely represented nongrowing populations. Dominant T-RFs were 3–4 bp shorter than those predicted for related clones in the inoculum. This variation has been observed in several previous studies (Kitts 2001), and Kaplan & Kitts (2003) compared detected T-RFs to actual ones for 21 bacterial species and found detected lengths varied from predictions by an average of −3 bp.

Soluble U(VI) decreased concurrently with sulfate in many microcosms, and it is therefore

likely that sulfate-reducing bacteria contributed to U(VI) reduction. Soluble U(VI) only rebounded in those microcosms in which sulfate and acetate were depleted, suggesting a limitation to the activity of sulfate-reducing bacteria in these vials. A TAP T-RFLP analysis correlated six species of known sulfate-reducing bacteria to T-RFs that appeared during the course of the experiment. Five of these were of the genera *Desulfovibrio*. Members of this genera are known to reduce U(VI) (Lovley et al. 1993). Most iron remained oxidized in this experiment. Though Fe(III) reduction ($E^{\circ\prime} = 0.20$ V) is thermodynamically favored over sulfate reduction ($E^{\circ\prime} = -0.217$ V), soluble sulfate may have been more bioavailable than solid-phase Fe(III), or the original inoculum may have contained more sulfate- than Fe(III)-reducing bacteria.

Fermenting bacteria may also have reduced U(VI). The greater decline in pH in viable than control microcosms is consistent with fermentation. *Clostridium* species have T-RFs of the same length as those that appeared during the course of the experiment. A *Clostridium* species was reported to reduce U(VI) in previous work (Francis et al. 1994). In some samples taken on Day 93, acetate accumulated to a greater stoichiometric concentration than the initial ethanol concentration, suggesting homoacetogenic production of acetic acid. Homoacetogenic bacteria have also been shown to reduce U(VI), but only in the absence of bicarbonate (Suzuki et al. 2004). Additional study is needed to determine to what degree these processes may have contributed to the observed reduction of uranium.

Rate control on aqueous U(VI) concentration

The soluble concentration of U(VI) in quiescent systems is controlled by the relative rates of sorption/desorption and biological or chemical transformation (Nyman et al. 2005). An increase in soluble U(VI) concentration can be expected when rates of desorption and solubilization exceed rates of reduction and sorption. In this work, U(VI) concentrations rebounded in microcosms that became depleted in sulfate, acetate, and ethanol. Both desorption and reoxidation likely contributed to this rebound. The sediment was a significant reservoir of U(VI) and as biological reduction rates decreased due to substrate limitation solid-phase U(VI) likely desorbed to maintain equilibrium. Sorption/desorption is also affected by solution pH. The pH in rebound microcosms was higher than in most other viable microcosms (Figure 2), likely because of acetate consumption or sulfate reduction. Since U(VI) sorption decreases above pH 6 (Barnett et al. 2002), the pH increase likely contributed to the higher final U(VI) concentration in rebound microcosms. In addition to desorption, U(IV) may have been reoxidized by ferric iron. Sani et al. (2004) observed a rebound in soluble U(VI) concentration in their systems, and suggested that as sulfate-reducing bacteria became limited by electron donor availability, Fe(III)-(hydr)oxides reoxidized U(IV). These findings have two important implications: U(VI) reduction rates in the field will depend upon adequate delivery and mixing of electron donors and acceptors during bioremediation, and long-term chemical delivery may be required to maintain microbial activity for the immobilization of uranium.

Small-scale heterogeneity

Variation in chemical transformations among replicate microcosms indicated that small-scale community and/or mineralogical heterogeneity influenced U(VI) reduction patterns. Soluble U(VI) rebounded in some microcosms, while in others soluble U(VI) concentration continually decreased or leveled off. Acetate and sulfate were depleted in vials with rebounding U(VI), but in others acetate persisted and sulfate was only partially consumed. Though the pool of sediment was well-mixed during the experimental setup, microscale variations in composition still apparently influenced U(VI) behavior. The initial mass of solid-phase U(VI) may have differed between microcosms, for example, or the type and amount of minerals with U(VI) sorption sites may have varied between vials. Moreover, sediment structure that developed in the microcosms may have resulted in microenvironments that differed between replicates.

In addition to heterogeneity in the solid phase, microbial communities certainly diverged over time with respect to minor members, and this divergence may have resulted in variation in observed chemical reactions. Swenson et al. (2000) recognized microbial communities as complex

systems that are highly sensitive to initial conditions. They suggested even small differences between replicates can result in large differences in community structure and function with time, a property they used for ecosystem-level selection of biodegradative communities. Variable function from replicate sediment inocula has also been observed previously. Arias & Tebo (2003) developed duplicate, Cr(VI)-reducing enrichments from sediment with sulfate as an electron acceptor, and while one was sulfidogenic, the other was not. Differences in chemical reactions between microcosms implies localized variation in microbial activity on a small scale, possibly as a result of divergent development of community structure.

The observed function of U(VI) reduction varied significantly between replicates due to heterogeneity, suggesting field-scale analysis may be a composite of multiple types and rates of reactions within microenvironments. This finding indicates a need for high-resolution sampling and fine-scale analysis in the identification and quantification of desorption and reaction mechanisms. The observations of heterogeneity and the rebound in soluble U(VI) concentration highlight the importance of elucidating serial and parallel rates of sorption/desorption, abiotic transformation, and biotic transformation (Nyman et al. 2005).

Acknowledgements

This work was funded from the National Science Foundation graduate fellowship program and a United States Department of Energy (DOE) Natural and Accelerated Bioremediation Research (NABIR) Biological and Environmental Research (BER) grant (#DE-F603-00ER63046). The authors would like to thank David Watson of the Oak Ridge Field Research Center for providing sediment samples, and Dr. Wei-Min Wu for providing denitrified synthetic groundwater. Portions of this research were carried out at the Stanford Synchrotron Radiation Laboratory, a national user facility operated by Stanford University on behalf of the United States Department of Energy, Office of Basic Energy Sciences. The SSRL Structural Molecular Biology Program is supported by the Department of Energy, Office of Biological and Environmental Research, and by the National Institutes of Health, National Center for Research Resources, Biomedical Technology Program. Other portions were performed at GeoSoilEnviroCARS (Sector 13), Advanced Photon Source (APS), Argonne National Laboratory. GeoSoilEnviroCARS is supported by the National Science Foundation – Earth Sciences (EAR-0217473), Department of Energy – Geosciences (DE-FG02-94ER14466) and the State of Illinois. Use of the APS was supported by the US Department of Energy, Basic Energy Sciences, Office of Energy Research, under Contract No. W-31-109-Eng-38.

References

Abdelouas A, Lu YM, Lutze W & Nuttall HE (1998) Reduction of U(VI) to U(IV) by indigenous bacteria in contaminated ground water. J. Contam. Hydrol. 35: 217–233

Anderson RT, Vrionis HA, Ortiz-Bernad I, Resch CT, Long PE, Dayvault R, Karp K, Marutzky S, Metzler DR, Peacock A, White DC, Lowe M & Lovley DR (2003) Stimulating the *in situ* activity of *Geobacter* species to remove uranium from the groundwater of a uranium-contaminated aquifer. Appl. Environ. Microbiol. 69: 5884–5891

Arias YM & Tebo BM (2003) Cr(VI) reduction by sulfidogenic and nonsulfidogenic microbial consortia. Appl. Environ. Microbiol. 69: 1847–1853

Barnett MO, Jardine PM & Brooks SC (2002) U(VI) adsorption to heterogeneous subsurface media: application of a surface complexation model. Environ. Sci. Technol. 36: 937–942

Bertsch PM, Hunter DB, Sutton SR, Bajt S & Rivers ML (1994) *In-situ* chemical speciation of uranium in soils and sediments by micro X-ray absorption spectroscopy. Environ. Sci. Technol. 28: 980–984

Brooks SC, Fredrickson JK, Carroll SL, Kennedy DW, Zachara JM, Plymale AE, Kelly SD, Kemner KM & Fendorf S (2003) Inhibition of bacterial U(VI) reduction by calcium. Environ. Sci. Technol. 37: 1850–1858

Coates JD, Chakraborty R, Lack JG, O'Connor SM, Cole KA, Bender KS & Achenbach LA (2001) Anaerobic benzene oxidation coupled to nitrate reduction in pure culture by two strains of *Dechloromonas*. Nature 411: 1039–1043

Cole JR, Chai B, Marsh TL, Farris RJ, Wang Q, Kulam SA, Chandra S, McGarrell DM, Schmidt TM, Garrity GM & Tiedje JM (2003) The Ribosomal Database Project (RDP-II): previewing a new autoaligner that allows regular updates and the new prokaryotic taxonomy. Nucleic Acids Res. 31: 442–443

Dunbar J, Ticknor LO & Kuske CR (2001) Phylogenetic specificity and reproducibility and new method for analysis of terminal restriction fragment profiles of 16S rRNA genes from bacterial communities. Appl. Environ. Microbiol. 67: 190–197

Elias DA, Senko JM & Krumholz LR (2003) A procedure for quantitation of total oxidized uranium for bioremediation studies. J. Microbiol. Methods 53: 343–353

Finneran K, Housewright M & Lovley D (2002a) Multiple influences of nitrate on uranium solubility during bioremediation of uranium-contaminated subsurface sediments. Environ. Microbiol. 4: 510–516

Finneran KT, Anderson RT, Nevin KP & Lovley DR (2002b) Potential for bioremediation of uranium-contaminated aquifers with microbial U(VI) reduction. Soil Sediment Contam. 11: 339–357

Francis AJ, Dodge CJ, Lu FL, Halada GP & Clayton CR (1994) XPS and XANES studies of uranium reduction by *Clostridium* sp. Environ. Sci. Technol. 28: 636–639

Gentile M, Yan TF, Tiquia S, Fields M, Nyman J, Zhou J & Criddle C (2005) Stability in a denitrifying fluidized bed reactor. Microbiol Ecology (forthcoming)

Gorby Y & Lovley D (1992) Enzymatic uranium precipitation. Environ. Sci. Technol. 26: 205–207

Istok JD, Senko JM, Krumholz LR, Watson D, Bogle MA, Peacock A, Chang YJ & White DC (2004) *In situ* bioreduction of technetium and uranium in a nitrate-contaminated aquifer. Environ. Sci. Technol. 38: 468–475

Kaplan CW & Kitts CL (2003) Variation between observed and true Terminal Restriction Fragment length is dependent on true TRF length and purine content. J. Microbiol. Methods 54: 121–125

Kitts CL (2001) Terminal Restriction Fragment patterns: a tool for comparing microbial communities and assessing community dynamics. Curr. Issues Intest. Microbiol. 2: 17–25

Kemner KM, Kelly SD, Orlandini KA, Tsapin AI, Goldfeld MG, Perfiliev YD & Nealson KH (2001) XAS investigations of Fe(VI). J. Synchrotron Radiat. 8: 949–951

Kniemeyer O, Probian C, Rossello-Mora R & Harder J (1999) Anaerobic mineralization of quaternary carbon atoms: isolation of denitrifying bacteria on dimethylmalonate. Appl. Environ. Microbiol. 65: 3319–3324

Lane DJ (1991) 16S/23S rRNA sequencing. In: Stackebrandt E & Goodfellow M (Eds) Nucleic Acid Techniques in Bacterial Systematics, (pp 115–175). John Wiley & Sons Ltd, Chichester, England

Lovley DR, Phillips EJP, Gorby YA & Landa ER (1991) Microbial reduction of uranium. Nature 350: 413–416

Lovley DR, Roden EE, Phillips EJP & Woodward JC (1993) Enzymatic iron and uranium reduction by sulfate-reducing bacteria. Mar. Geol. 113: 41–53

Lytle FW, Greego RB, Sandston DR, Marques EC, Wong J, Spiro CL, Huffman GP & Huggins FE (1984) Measurements of soft X-ray absorption spectra with a fluorescent ion chamber. Nucl. Instrum. Methods Phys. Res. Sect. A 226: 542–548

Marsh TL, Saxman P, Cole J & Tiedje J (2000) Terminal restriction fragment length polymorphism analysis program, a web-based research tool for microbial community analysis. Appl. Environ. Microbiol. 66: 3616–3620

Myers CR & Nealson KH (1988) Bacterial manganese reduction and growth with manganese oxide as the sole electron acceptor. Science 240: 1319–1321

Nevin KP, Finneran KT & Lovley DR (2003) Microorganisms associated with uranium bioremediation in a high-salinity subsurface sediment. Appl. Environ. Microbiol. 69: 3672–3675

Newville M (2001) IFEFFIT: interactive XAFS analysis and FEFF fitting. J. Synchrotron Radiat. 8: 322–324

Nyman JL, Williams SM & Criddle CS (2005) Bioengineering for the *in-situ* remediation of metals. In: Grassian VH (Ed) Environmental Catalysis. (pp 493–520) Taylor & Francis Boca Raton, FL

Patterson RR, Fendorf S & Fendorf M (1997) Reduction of hexavalent chromium by amorphous iron sulfide. Environ. Sci. Technol. 31: 2039–2044

Peterson ML, White AF, Brown GE & Parks GA (1997) Surface passivation of magnetite by reaction with aqueous Cr(VI): XAFS and TEM results. Environ. Sci. Technol. 31: 1573–1576

Ressler T, Wong J, Roos J & Smith IL (2000) Quantitative speciation of Mn-bearing particulates emitted from autos burning (methylcyclopentadienyl)manganese tricarbonyl-added gasolines using XANES spectroscopy. Environ. Sci. Technol. 34: 950–958

Riley RG, Zachara JM & Wobber FJ (1992) Chemical Contaminants on DOE Lands and Selection of Contaminant Mixtures for Subsurface Science Research. Report No. DOE/ER-0547T, Office of Energy Research, US Department of Energy, Washington, DC

Sani RK, Peyton BM, Amonette JE & Geesey GG (2004) Reduction of uranium(VI) under sulfate-reducing conditions in the presence of Fe(III)-(hydr)oxides. Geochim. Cosmochim. Acta 68: 2639–2648

Schulze R, Spring S, Amann R, Huber I, Ludwig W, Schleifer KH & Kampfer P (1999) Genotypic diversity of *Acidovorax* strains isolated from activated sludge and description of *Acidovorax defluvii* sp. nov. Syst. Appl. Microbiol. 22: 205–214

Senko J, Istok J, Suflita J & Krumholz L (2002) *In-situ* evidence for uranium immobilization and remobilization. Environ. Sci. Technol. 36: 1491–1496

Shelobolina ES, O'Neill K, Finneran KT, Hayes LA & Lovley DR (2003) Potential for *in situ* bioremediation of a low-pH, high-nitrate uranium-contaminated groundwater. Soil Sediment Contam. 12: 865–884

Suzuki Y, Kelly SD, Kemner KA & Banfield JF (2003) Microbial populations stimulated for hexavalent uranium reduction in uranium mine sediment. Appl. Environ. Microbiol. 69: 1337–1346

Suzuki Y, Kelly SD, Kemner KM & Banfield JF (2004) Enzymatic U(VI) reduction by *Desulfosporosinus* species. Radiochim. Acta 92: 11–16

Swenson W, Arendt J & Wilson DS (2000) Artificial selection of microbial ecosystems for 3-chloroaniline biodegradation. Environ. Microbiol. 2: 564–571

Waychunas GA, Apted MJ & Brown GE (1983) X-ray K-edge absorption spectra of Fe minerals and model compounds: near-edge structure. Phys. Chem. Miner. 10: 1–9

Widdel F & Pfennig N (1984) Dissimilatory sulfate- or sulfur-reducing bacteria. In: Krieg NR & Holt JG (Eds) Bergey's Manual of Systematic Bacteriology, Vol. 1 (pp 663–679). Williams and Wilkins, Baltimore, MD